Equatorial Ionospheric Electric Fields During the November 2004 Magnetic Storm

B. G. Fejer,[1] J. W. Jensen,[1] T. Kikuchi,[2] M. A. Abdu,[3] and J. L. Chau[4]

Received 27 February 2007; revised 28 June 2007; accepted 10 August 2007; published 16 October 2007.

[1] We use radar measurements from the Jicamarca Radio Observatory, magnetometer observations from the Pacific sector and ionosonde data from Brazil to study equatorial ionospheric electric fields during the November 2004 geomagnetic storm. Our data show very large eastward and westward daytime electrojet current perturbations with lifetimes of about an hour (indicative of undershielding and overshielding prompt penetration electric fields) in the Pacific equatorial region during the November 7 main phase of the storm, when the southward IMF, the solar wind and reconnection electric fields, and the polar cap potential drops had very large and nearly steady values. This result is inconsistent with the recent suggestion that solar wind electric fields penetrate without attenuation into the equatorial ionosphere for several hours during storm main phase. The largest daytime prompt penetration electric fields (about 3 mV/m) ever observed over Jicamarca occurred during the November 9 storm main phase, when large equatorial electrojet current and drift perturbations were also present in the Pacific and Brazilian equatorial regions. The rise and decay times of these equatorial electric fields were about 20 min longer than of the corresponding solar wind electric fields. The ratios of prompt penetration electric fields and corresponding solar wind electric field changes were highly variable even during the day, and had largest values near dawn. Also, the prompt penetration electric fields did not show polar cap potential drop saturation effects. Our results clearly highlight that the relationships of prompt penetration and solar wind electric fields, and polar cap potentials are far more complex than implied by simple proportionality factors.

Citation: Fejer, B. G., J. W. Jensen, T. Kikuchi, M. A. Abdu, and J. L. Chau (2007), Equatorial Ionospheric Electric Fields During the November 2004 Magnetic Storm, *J. Geophys. Res.*, *112*, A10304, doi:10.1029/2007JA012376.

1. Introduction

[2] Low latitude ionospheric electric fields and currents have been the subject of numerous investigations [e.g., *Kelley*, 1989; *Abdu et al.*, 1995; *Fejer*, 1997; *Sastri et al.*, 1997; *Buonsanto*, 1999; *Kikuchi et al.*, 2000, 2003]. Radar and satellite plasma drift and ground based magnetic field measurements have determined the average ionospheric plasma drift (electric field) and current patterns during quiet times, and their climatological responses to enhanced geomagnetic activity [e.g., *Fejer*, 1997, 2004], and theoretical and modeling studies have identified the main quiet and storm-time driving mechanisms. It is now well established that low latitude ionospheric plasma drift and current perturbations during geomagnetically active times are due mostly to the combined effects of relatively short-lived prompt penetration and longer lasting ionospheric disturbance dynamo electric fields.

[3] Prompt penetration electric fields occur predominantly during periods of large and rapid IMF driven changes in magnetospheric convection, when there is a temporary imbalance between the convection-related charge density and the charge density in the Alfvén layer. These electric fields can also be explained as resulting from changes in the relative strengths of the region 1 and region 2 Birkeland currents. During periods of sudden increases (decreases) in convection, the nighttime shielding layer moves equatorward (poleward) and the temporary undershielding (overshielding) of the inner magnetosphere generates a dawn-dusk (dusk-dawn) transient electric field [e.g., *Wolf*, 1983; *Senior and Blanc*, 1984; *Spiro et al.*, 1988; *Fejer et al.*, 1990; *Peymirat et al.*, 2000]. These transient electric fields have typical rise and decay times shorter than about 15 min, and lifetimes of about an hour [e.g., *Gonzales et al.*, 1979; *Fejer*, 1986; *Fejer and Scherliess*, 1997]. They disturb the ionosphere nearly simultaneously from middle to equatorial latitudes [e.g., *Kikuchi et al.*, 1996, 2000]. Recently, an excellent review of large scale convection electric fields in the inner

[1]Center for Atmospheric and Space Science, Utah State University, Logan, Utah, USA.
[2]Solar Terrestrial Environment Laboratory, Nagoya University, Nagoya, Aichi, Japan.
[3]Instituto de Pesquisas Espaciais, Sao Paulo, Brazil.
[4]Radio Observatorio de Jicamarca, Instituto Geofisico del Peru, Peru.

0148-0227/07/2007JA012376

magnetosphere and undershielding and overshielding effects was published by *Wolf et al.* [2007].

[4] Ionospheric prompt penetration electric fields depend mostly on the solar wind and magnetospheric driving mechanisms, on the potential distribution penetrating to middle and low latitudes, and on the global distribution of ionospheric conductance. Average empirical equatorial prompt penetration electric fields are in good agreement with the predictions from global convection models [e.g., *Fejer and Scherliess*, 1997; *Fejer and Emmert*, 2003]. On the other hand, the large variability of these electric fields is not well understood [e.g., *Fejer*, 2002; *Huang et al.*, 2005], which indicates that their magnitudes and lifetimes are also affected by additional solar wind, magnetospheric, and high and low latitude ionospheric processes [e.g., *Spiro et al.*, 1988; *Peymirat et al.*, 2000; *Fejer*, 2004], whose effects tend to be averaged out in climatological studies.

[5] Ionospheric disturbance dynamo electric fields, with timescales from a few to several hours, are driven by enhanced energy deposition into the high latitude ionosphere [*Blanc and Richmond*, 1980]. Relatively fast (occurring about 2–3 h after major increases in convection) disturbance dynamo electric fields [e.g., *Scherliess and Fejer*, 1997] are most likely due to the dynamo action of fast traveling equatorward wind surges [e.g., *Fuller-Rowell et al.*, 2002], while slower disturbances (occurring 3–12 h later) are believed to be driven mostly by the electrodynamic action of storm-enhanced high latitude equatorward winds [*Blanc and Richmond*, 1980]. Disturbance dynamo perturbation electric fields occurring about one day after major enhancement in geomagnetic activity [*Scherliess and Fejer*, 1997] are most likely due to the combined effects of storm-driven equatorward winds and conductivity variations, resulting from storm driven ionospheric composition changes. The low latitude ionospheric disturbance dynamo electric fields are westward during the day and eastward at night, with largest magnitudes in the late night sector [*Scherliess and Fejer*, 1997]. Although the climatological disturbance dynamo electric fields are in good agreement with the predictions from the Blanc-Richmond model, their large spatial and temporal variability [e.g., *Fejer*, 2002; *Su et al.*, 2003] still remains to be understood.

[6] Recent studies have shown that very large spatial- and temporal-dependent changes in the middle and low latitude ionospheric plasma density distribution during large geomagnetic storms are associated with unusually large enhancements in the low latitude daytime eastward electric fields [e.g., *Basu et al.*, 2001; *Sastri et al.*, 2002]. These studies have motivated an increased interest in storm-time equatorial electric fields. *Kelley et al.* [2003] used ACE solar wind data and Jicamarca vertical drifts during 15–18 April 2002 to show that, for periods less than about 2 h, the ratio of the interplanetary and equatorial dawn-to-dusk electric field components was about 15:1. *Maruyama et al.* [2005] have pointed out the importance of a feedback between prompt penetration and disturbance dynamo electric fields, and *Huang et al.* [2005] suggested that, the interplanetary electric field can continuously penetrate to the low latitude ionosphere without shielding during storm periods of strengthening geomagnetic activity. Recently, *Huang et al.* [2007] derived an average ratio of about 10:1 between the zonal electric fields derived from solar wind and from Jicamarca vertical drift observations.

[7] In this work, we use vertical plasma drift observations from the Jicamarca Radio Observatory (11.9°S, 76.8°W, dip latitude 1°N), magnetometer measurements from Peru and from the 210° magnetic meridian sector, and ionosonde data from Brazil during the large magnetic storm of 7–12 November 2004 to study the characteristics of storm-time equatorial zonal electric field perturbations, and their relationship to solar wind and magnetospheric parameters. Our data show the occurrence of large overshielding electric fields even during the main phase of the storm, when the IMF was strongly southward. They also show that nighttime disturbance dynamo effects dominate over prompt penetration electric fields effects during periods of very large, nearly steady, solar wind eastward electric fields and polar cap potential drops, and highlight the transient nature of the equatorial prompt penetration electric fields. These results indicate that the physics of equatorial storm-time prompt penetration electric fields is far more complex than implied by a simple proportionality factor between equatorial ionospheric and solar wind electric fields and magnetospheric currents.

2. Data

[8] We have used solar wind plasma and magnetic field measurements from the SWEPAM and MAG instruments on board the ACE satellite. We have also examined the solar wind and magnetic field data from the SWE and MFI probes on the WIND satellite, but these data will not be shown here. The ACE and WIND data were obtained from the NASA/GSFC CDAWeb site. These measurements were used to calculate the solar wind and reconnection electric fields and, together with the decimetric solar flux index, also the polar cap potential drop.

[9] We used two geomagnetic indices, *SYM-H* and *ASY-H* [*Iyemori*, 1990; *Iyemori and Rao*, 1996], as indicators of the level of geomagnetic activity. The *SYM-H* index is the average of the H-component from six, primarily midlatitude, stations and corresponds to the symmetric component of the northward geomagnetic field variations. This parameter gives essentially the same information on the strength of the symmetric ring current as the hourly *Dst* index, but with a 1-min time resolution. The *ASY-H* index is generally well correlated with *AE* index, but does not reflect accurately the occurrence of substorms.

[10] Equatorial zonal electric fields were obtained from vertical plasma drift observations at the Jicamarca Radio Observatory. From about 0900 and 1600 LT (1400 and 2100 UT) on 7 November, these drifts were measured with a 5-min time resolution using Doppler observations of 150 km radar echoes detected by the JULIA (Jicamarca Unattended Long-Term Ionosphere Atmosphere Radar) system [*Kudeki and Fawcett*, 1993; *Woodman and Villanueva*, 1995]. Incoherent scatter radar *F* region vertical drift measurements were made from 1150 LT 9 November to 1200 LT 14 November with an integration time of 5-min using the experimental procedure developed by *Woodman* [1970], and the data acquisition and signal processing techniques described by *Kudeki et al.* [1999]. Since the vertical drifts generally do not change much with height

[e.g., *Woodman*, 1970], most of our results correspond to averages over the altitudinal range of about 240-600 km, where the signal-to-noise ratios are highest. During periods of strong equatorial spread *F*, the height range of drift measurements was changed (extending sometimes up to about 850 km) to minimize the effects of these strong coherent echoes. These drifts cannot be accurately measured when strong spread *F* echoes occur over most of the altitudes sampled by the radar. The accuracy of the drift measurements varied typically from about 1 m/s during the day to about 10 m/s in the late nighttime period. At *F* region heights over Jicamarca, an upward drift velocity of 40 m/s corresponds to an eastward electric field of about 1 mV/m.

[11] Several studies have shown that simultaneous measurements of the horizontal (northward) component of the Earth's magnetic field at equatorial and off equatorial stations in nearly the same longitudinal sector can be used to estimate daytime *F* region equatorial vertical plasma drifts (zonal electric fields) [e.g., *Anderson et al.*, 2002]. Therefore we have complemented the radar drift measurements with ground-based magnetic field observations from Jicamarca and Piura (5.17° S, 80.64° W, geomagnetic latitude 6.81°) in the Peruvian equatorial region, and from Yap (9.30° N, 138.50° E, dip latitude 0.30°) and Okinawa (26.75° N, 128.22° E, geomagnetic latitude 26.75°) in the Pacific region. We estimate that during November 2004 an eastward electric field of 1 mV/m corresponds to ΔH (Yap-Okinawa) = 140 nT at noon (0300 UT), and to about 70 nT at 0900 and 1400 LT. We have also examined the magnetic field data from Guam (13.58°N, 144.78°E, dip latitude 4.5°), but they will not be presented them here, since ΔH (Yap-Guam) gave essentially identical ionospheric perturbations currents as obtained from the Yap and Okinawa data.

[12] Nighttime equatorial vertical plasma drifts can also be inferred from ionosonde observations of the time rate of change of the height of the bottomside of the *F* layer ($h'F$), when this bottomside is above 300 km [*Bittencourt and Abdu*, 1981], which is most often the case near dusk. We have also used ionosonde measurements from Saõ Luís (2.3° S, 44.2° W, dip latitude 0.3° S) to estimate the evening vertical perturbation drifts over the Brazilian equatorial region during this storm, and to determine their relationship to the equatorial zonal disturbance electric fields observed in the Pacific and Peruvian sectors.

3. Results

[13] In this section we describe initially the general characteristics of the main solar wind and magnetospheric parameters during the November 2004 storm, which are then used to derive the solar wind and reconnection electric fields and the polar cap potential drops. Then, we describe the equatorial zonal electric fields derived from vertical plasma drift, electrojet current and ionosonde measurements, and examine their relationships to the solar wind electric fields and magnetospheric convection.

3.1. Solar Wind and Magnetospheric Conditions

[14] November 7–12, 2004 was a period of declining solar flux with an average decimetric index of about 110, but with strong geomagnetic activity. Figure 1 presents, in the top panels, the solar wind speed, dynamic pressure ($P_{SW} = nm_P V_{SW}^2$, where n is the solar wind number density and m_P is the proton mass), and the IMF *By* and *Bz* components during November 7–10 measured by the ACE satellite, which was located at about (242, 24, −16) R_E in GSE coordinates. These data have been delayed to their interaction time at the magnetopause. Nearly identical values were measured by the WIND satellite at about (200, 57, −8) R_E. The bottom panels show the *ASY-H* and *SYM-H* indices.

[15] Figure 1 shows that the solar wind speed increased gradually from about 400 km/s to about 500 km/s from 1200 to 1800 UT on 7 November, and then abruptly to 650 km/s at the storm sudden commencement at about 1900 UT. Later, it gradually decreased to about 600 km/s before increasing again to about 800 km/s at 0900 UT on 9 November. There was another solar wind speed increase with simultaneous increase in the solar wind dynamic pressure at about 1800 UT on the 9th. In this period, there were also very large changes in the solar wind dynamic pressure (up to about 60 nPa), and large IMF*Bz* and IMF*By* values (up to about 50 nT). *SYM-H* reached a minimum value of −394 nT at 0556 UT on 8 November, and had secondary minima of about −280 nT at 2104 UT on the 9th, and 0932 UT on the 10th, with moderately active conditions between these most disturbed times.

[16] We have studied the characteristics of equatorial plasma drifts and current disturbances during this highly disturbed period, and their relationship to the solar wind and reconnection electric fields, and polar cap potential drop. We define the zonal component of the motional solar wind electric field E_y (mV/m) = $V_{SW}B_Z$, where V_{SW}(km/s) is the solar wind speed, and B_Z(nT) is the north-south component of the IMF in GSM coordinates, and the reconnection electric field E_R (mV/m) = $V_{SW}B\sin^2(\theta/2)$, where B(nT) is the Y-Z plane component of the IMF in GSM coordinates, and θ is the IMF clock angle in the Y-Z plane, with 0° and 180° being northward and southward, respectively.

[17] Following *Ober et al.* [2003], we calculated the polar cap potential drop (transpolar potential) using the Hill-Siscoe polar cap formula [e.g., *Siscoe et al.*, 2002]. This potential, which includes a 30 kV potential to account for viscous merging and predicts saturation for large solar wind reconnection electric fields, is given by

$$\Phi_{PC}(\mathrm{kV}) = \frac{30 + 57.6 E_R P_{sw}^{-1/6}}{1 + 0.020 \sum_p P_{sw}^{-1/3} + 0.036 E_R P_{sw}^{-1/2} \sum_p} \quad (1)$$

where E_R is the reconnection electric field, P_{SW} is the solar wind ram pressure in nPa, $\Sigma_P = 0.77(F_{10.7})^{1/2}$ is the height integrated Pedersen conductivity in S, $F_{10.7}$ is the solar decimetric flux index, and the other symbols have their usual meaning. This simple expression of the Pedersen conductivity neglects the contribution from particle precipitation, which might not be a good assumption during such a severe storm. We have also calculated the polar cap potential using the empirical relationship derived by *Boyle et al.* [1997] from DMSP and solar wind parameters, which is given by

$$\Phi_B(\mathrm{kV}) = 10^{-4} V_{sw}^2 + 11.7 B \sin^3(\theta/2) \quad (2)$$

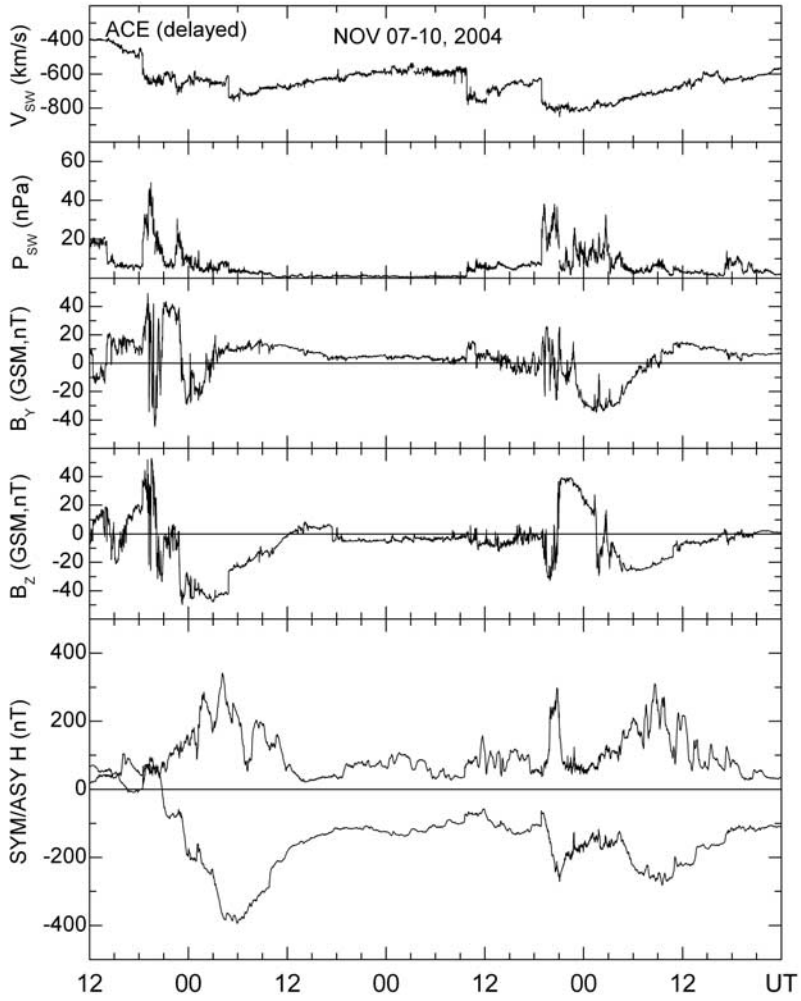

Figure 1. Solar wind speed, pressure, and IMF B_y and B_z measured by the ACE satellite and delayed to the interaction time to the magnetopause, and *SYM-H* and *ASY* indices during the 7–10 November 2004 magnetic storm.

where V_{SW} is the solar wind speed in km/s. The potential drop calculated using the latter formula will be shown only for the period of extremely strong prompt penetration electric field during 9 November.

3.2. Equatorial Ionospheric Observations

[18] Figure 2 presents in the top panels the solar wind and reconnection electric fields, the cross polar cap potential drop, and the *SYM-H* and *ASY-H* indices during 7–8 November. The bottom panels show the intensity of the equatorial electrojet over the Pacific equatorial station Yap estimated by subtracting the horizontal (northward) components over Yap and Okinawa, and the daytime vertical plasma drifts (i.e., zonal electric fields) over Jicamarca. The vertical drifts were obtained using Doppler radar measurements of 150-km echoes; near 1600 UT they were corrected using Jicamarca and Piura magnetic field data.

[19] Figure 2 shows short-lived upward perturbation drifts with peak values of 20 m/s at 1530 and 40 m/s at 1610 UT over Jicamarca prior to the storm main phase. These equatorial eastward electric fields of about 0.5 and 1 mV/m were associated with rapid changes of about 10 and 20 mV/m in the solar wind and reconnection electric fields, and about 100 kV in the polar cap potential drop. The upward drifts decreased rapidly between 1610 and 1625 UT, and more gradually later; they became downward at about 1650 UT and reached −15 m/s near 1750 UT. The slowly varying, relatively long-lived, downward perturbation drifts (westward electric fields) were most probably due to disturbance dynamo electric fields. The vertical drifts remained downward up to about 1825 UT, when there was a rapid upward drift perturbation of about 20 m/s (0.5 mV/m), probably resulting from the sudden compression of the magnetopause as indicated by *Sym-H*, which is seen more clearly in Figure 1.

[20] The Jicamarca data show a large (about 30 m/s) upward perturbation drift (eastward electric field at 0.75 mV/m) at about 2015 UT (1515 LT), associated with the rapid increase in the solar wind electric fields to 20 mV/m, and in the polar cap potential drop to 300 kV. Since the Pacific magnetometer stations were in the nightside at this time, they did not show noticeable current perturbations. After sunrise, however, they showed large westward current perturbations between about 2115 UT and 2215 UT (0615–0815 LT). Although the rapidly varying equatorial iono-

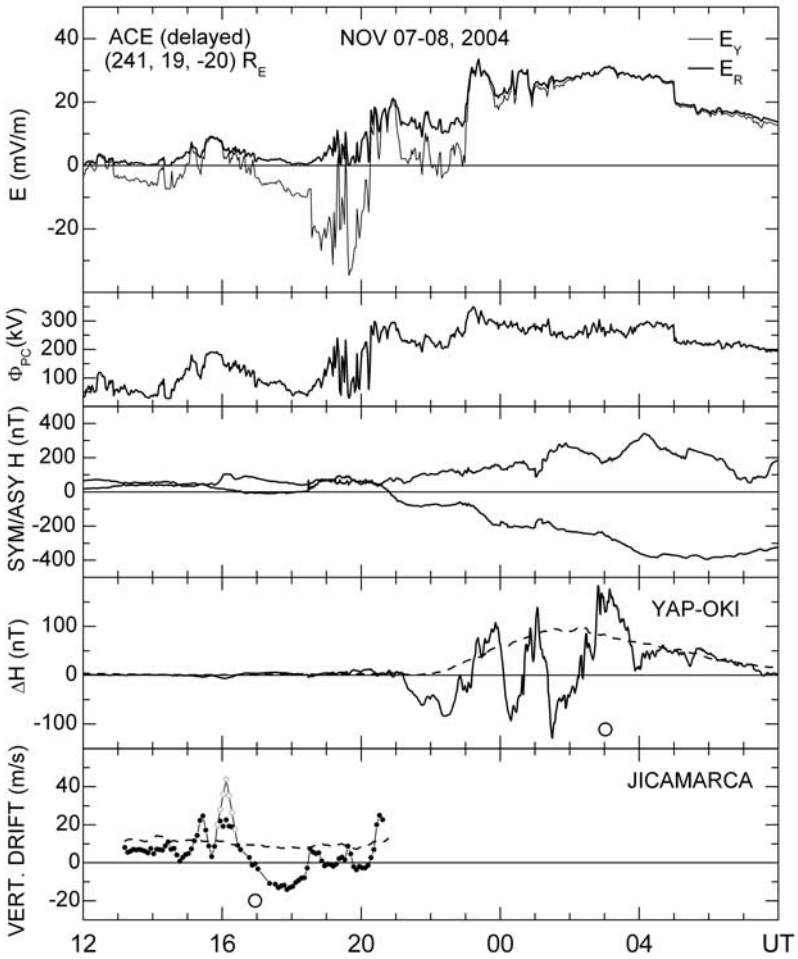

Figure 2. Solar wind, motional zonal electric fields, reconnection electric fields, polar cap potentials, *SYM-H* and *ASY* indices, equatorial magnetic field measurements over the Pacific and Jicamarca vertical plasma drifts during 7–8 November 2004. The small open circles in the Jicamarca data indicate velocities inferred from magnetometer data. The dashed curves denote the quiet time patterns, and the large circles indicate local noon.

spheric conductances near dawn preclude an accurate estimate of the magnitude of the electric field disturbances, these current perturbations are consistent with strong westward prompt penetration of electric fields at the beginning of the storm main phase. The magnetic field data also show very large positive current perturbations at 2300 and 0230 UT and negative perturbations at 2400 and 0100 UT. These are indicative of eastward and westward prompt penetration zonal electric fields of up to about 3 mV/m and with lifetimes of about 1-2 h, during the main phase of the storm, when the solar wind and the merging electric fields and the polar cap potential drops were mostly steady with values larger than about 30 mV/m and 200 kV, respectively. As mentioned earlier, nearly identical magnetic field perturbations were obtained using ΔH(YAP-Guam). These large magnetic field disturbances are somewhat related to changes in the time rate of change of the symmetric and asymmetric components of the *Dst* index, as indicated by the *SYM/ASY-H* indices. The São Luís ionosonde data also suggest the occurrence of large and short-lived vertical drifts perturbations during this period.

[21] The results shown in Figure 2 indicate that, as expected, rapid equatorial vertical drift perturbations closely follow large and rapid changes in both IMF *Bz* and polar cap potential drop. However, they also show that large magnitude, relatively short-lived eastward and westward prompt penetration equatorial electric field can occur during large and nearly steady southward IMF *Bz*, storm main phase periods, provided that ring current conditions are unsteady. This latter result is in contradiction with recent suggestions [e.g., *Huang et al.*, 2005] that the equatorial zonal electric fields follow the solar wind electric fields during storm main phase. Figure 2 also illustrates the occurrence of large overshielding electric fields at 2400 and 0100 UT in the absence of northward *Bz* turnings. Earlier examples of relatively short-lived overshielding-like equatorial electric fields during periods of large but unsteady southward IMF *Bz* were presented by *Fejer* [1986].

[22] Figure 3 shows in the top panels the solar wind and reconnection electric fields, the polar cap potential and the ring *SYM/ASY-H* indices; the bottom panels show equatorial electrojet magnetic field data from the Pacific sector, and the *F* region vertical drifts from Jicamarca during 9–

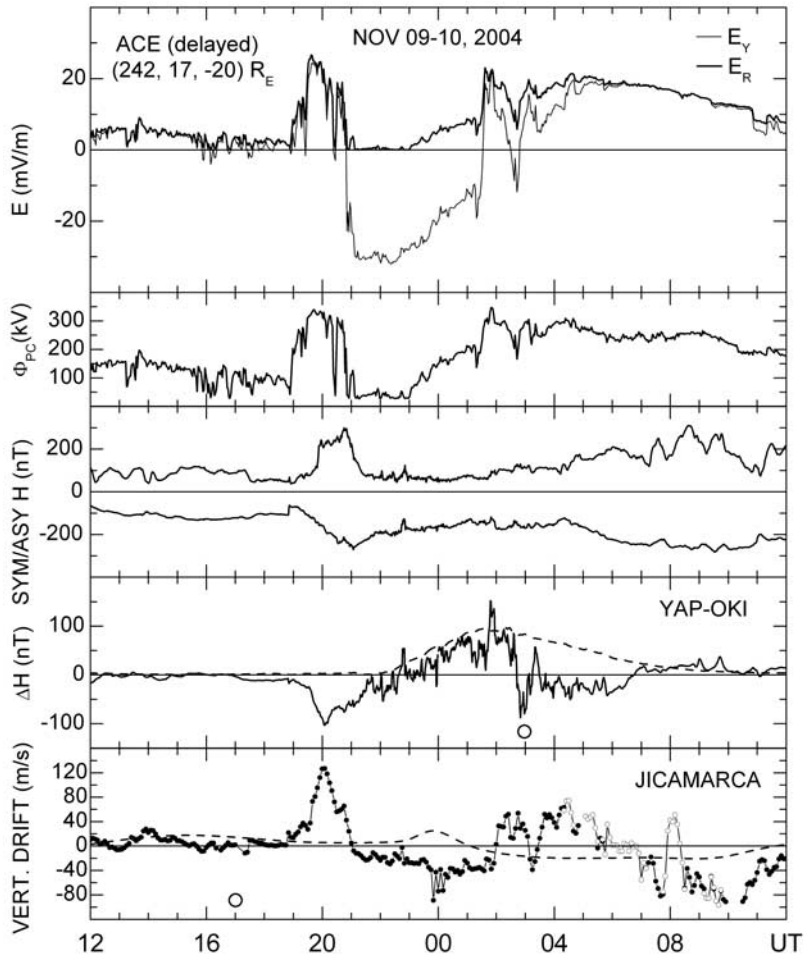

Figure 3. Same as Figure 2, but for 9–10 November 2004. The small circles in the Jicamarca data indicate plasma drifts measured over different height ranges due to the occurrence of strong spread F.

10 November 2004. The polar cap potentials shown in Figure 3 are in good agreement with calculations used to drive the Rice convection model (D. Wolf, private communication). We can see that between 1200 UT and the storm sudden commencement (SSC) at 1850 UT, geomagnetic activity was moderate with *SYM/ASY-H* values of about 100 nT, and that westward disturbance dynamo drifts were observed over Jicamarca.

[23] Figure 4 shows in more detail the data after the SSC, when there were first rapid and later more gradual increases of the solar wind electric fields to about 20 mV/m, and of the Hill-Siscoe and Boyle polar cap potential drops to about 300 and 400 kV, respectively. About half an hour later, these parameters underwent further rapid increases which led to a fast decrease of *SYM-H* and to a delayed large increase in *ASY-H*. Except for sharp brief decreases at 1920, 2008, and 2020 UT, the values of the solar wind and reconnection electric fields and polar cap potential drop remained very large and nearly steady until the onset of the storm recovery phase at about 2100 UT.

[24] Figure 4 indicates that following the storm sudden commencement, the Jicamarca upward drifts increased first rapidly to about 20 m/s, and then more gradually to about 40 m/s half an hour later. A much larger drift increase started at the onset of the storm main phase at about 1920 UT. In this case, the upward drifts reached about 120 m/s at 2000 UT (i.e., an eastward electric field of over 3 mV/m), which is the largest daytime value ever measured by the radar. During this period, the Pacific magnetic field data showed exceptionally large westward current perturbations, considering their occurrence close to dawn, which also maximized at about 2000 UT. Therefore these peak electric and magnetic field perturbations occurred about half an hour after the maximum values of the solar wind electric fields and polar cap potential drop, even though all these perturbations started at the same time. We should point out that the radar measurements had a time resolution of 5 min. The rapid changes in the solar wind electric fields and polar cap potential drops at about 2020 UT also led to much more gradual changes in the equatorial ionospheric magnetic and electric fields. Figure 4 clearly shows the ratio between the prompt penetration electric fields, responsible for vertical drift and magnetic field disturbances, and the solar wind and reconnection electric fields, and polar cap potentials changed markedly during this storm main phase. The ratio of the equatorial and solar wind electric fields, for example varied between about 0.05 and 0.12.

[25] The equatorial electric and magnetic fields decreased rapidly at about 2100 UT, following the sudden decease of the solar wind electric fields and polar cap potential drop

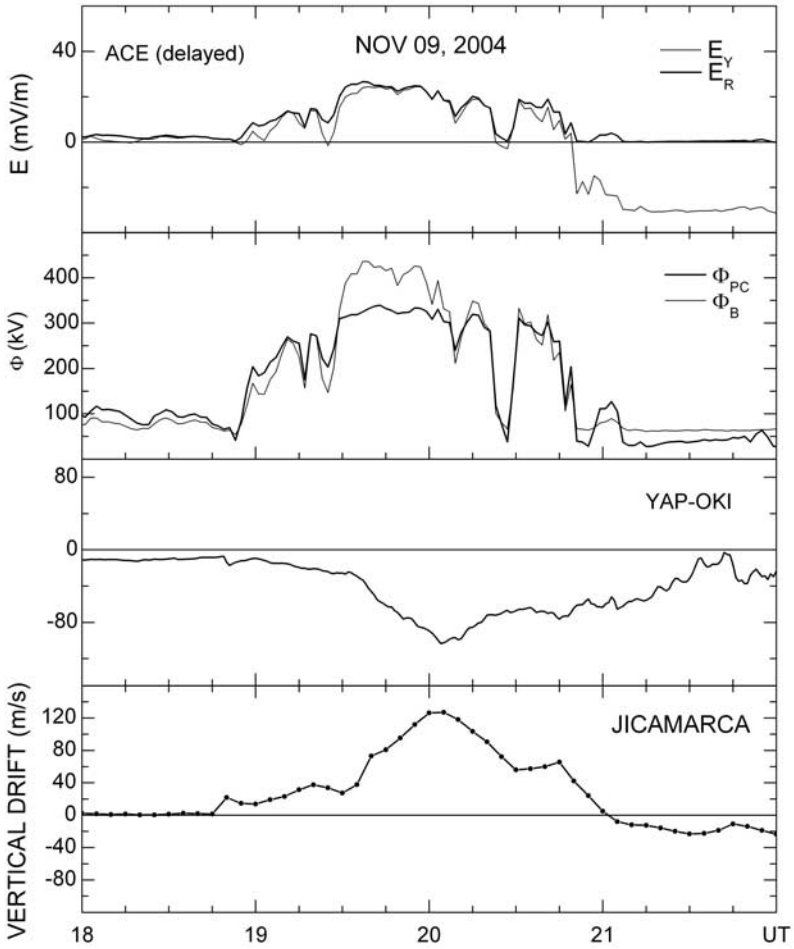

Figure 4. Solar wind electric fields, polar cap potential drops, equatorial magnetic fields, and Jicamarca vertical drifts during 18–22 UT on 9 November 2004.

and onset of the storm recovery phase. Figure 3 shows relatively large downward perturbation drifts from about 2100 to 0130 UT, while the corresponding magnetometer data generally followed the quiet time pattern, except for rapid perturbations. This indicates that even though the initial decrease of the Jicamarca downward drifts was due to prompt penetration electric fields, the longer lasting downward drifts after about 2200 UT were mostly due to westward disturbance dynamo electric fields, since prompt penetration electric fields would have driven much larger decreases in dayside ΔH than shown in the magnetometer data. Large electrodynamic disturbances were again observed between about 0130 and 0700 UT both in the Pacific and Peruvian equatorial regions, as shown in Figure 3. In this case, the Jicamarca data show predominantly upward perturbation drifts (eastward electric fields), except for large and short-lived superposed perturbations during times of rapid changes in the solar wind electric fields and polar cap potential drops. The corresponding short-lived magnetic field perturbations had opposite polarity to those over Jicamarca, as expected from prompt penetration electric fields. We should note that prompt penetration electric fields change polarity near dusk (about 0000–0100 UT over Jicamarca) [*Fejer et al.*, 1990].

[26] Figure 3 show large upward drift velocities and westward current perturbations during 0400–0700 UT, which was a period of very large and nearly steady solar wind and reconnection electric fields, polar cap potentials, and decreasing *Dst* values. This indicates that, except for brief periods of rapid variations in either the solar wind or magnetospheric drivers, the equatorial prompt penetration electric fields were either absent or much smaller than the disturbance dynamo electric fields, in spite of the very strong high latitude convection. Finally, large and short-lived velocity perturbations occurred over Jicamarca between about 0700 and 0900 UT (0200–0400 LT). In this case again, the solar wind electric field and polar cap potential were large and steady, but there were large variations in *ASY-H* which is indicative of large changes in the magnitude of high latitude potential penetrating equatorward of the shielding layer. Several earlier studies have illustrated the occurrence of overshielding electric fields following a weakening of the ring current [e.g., *Gonzales et al.*, 1979; *Fejer*, 1986].

[27] The large storm-induced electric field perturbations during November 7 and 9 discussed above were expected to produce large ionospheric disturbances in other longitudinal sectors also. These perturbations can be inferred from ionosonde measurements of the time rate of change of $h'F$, when $h'F$ is above about 300 km [*Bittencourt and Abdu*, 1981]. These ionosonde derived vertical drifts are most accurate after about 1800 LT (2100 UT). Figure 5

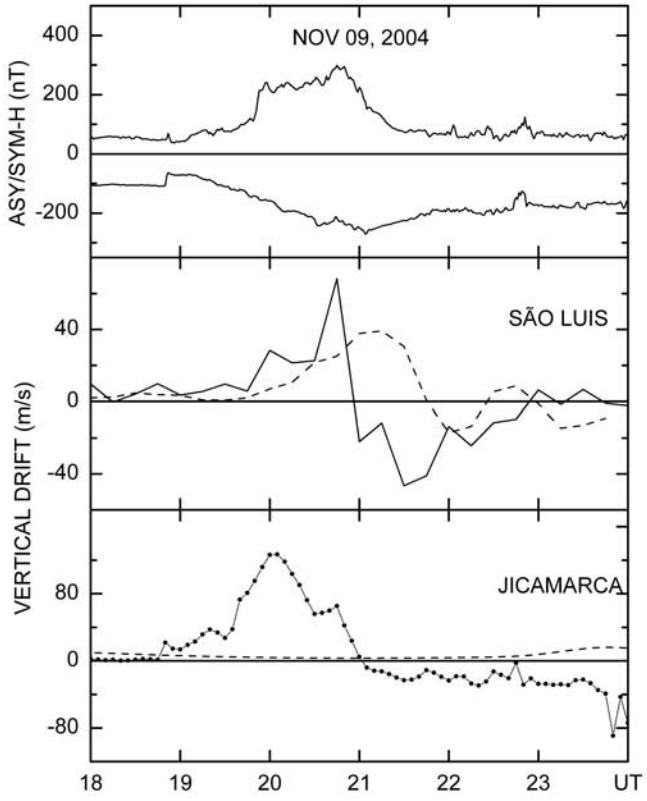

Figure 5. *SYM-H* and *ASY* indices, Brazilian ionosonde derived drifts and Jicamarca radar drifts during 9 November 2004. Over São Luís 21 UT corresponds to 18 LT. The dashed curves denote the quiet time patterns.

presents equatorial vertical plasma drifts inferred from ionosonde measurements over Saõ Luís, Brazil (2.33°S, 44.2°W; dip latitude 0.25°S) during November 9, together with the corresponding *ASY* and *SYM-H* indices, and Jicamarca vertical drifts. This Figure shows that the large ionosonde perturbation drifts over Brazil between about 1730 and 1900 LT (2030 and 2200 UT) are consistent with the corresponding Jicamarca data.

[28] We have seen that large prompt penetration and disturbance dynamo equatorial electric fields were observed during periods of very strong solar wind and magnetospheric driving conditions on 7–9 November. Figure 6 illustrates the occurrence of very large disturbance dynamo and prompt penetration electric fields during a period of significantly weaker solar wind and magnetospheric driving conditions during 11–12 November . In this case, the Jicamarca vertical plasma drifts were fairly close to their average quiet time values up to about 0300 UT (2200 LT), except for the larger evening prereversal enhancement at 2400 UT. Figure 6 shows disturbance dynamo upward drifts of about 40 m/s, between 0530 and 0730 UT, when the solar wind electric fields, polar cap potential drops, and *Dst* indices had relatively small values. This Figure also shows large magnitude and short-lived prompt penetration downward drift perturbations of 40 m/s and 80 m/s (westward electric fields of about 1 mV/m and 1.3 mV/m, respectively) centered at about 0830 and 0930 UT, during a period of small *Dst* decrease. These events are clearly associated with increases in the solar wind electric field and polar cap potential by about 4–5 mV/m and 80–110 kV, respectively. It should be noticed that the ratios of these early morning prompt penetration electric fields and the corresponding changes in the interplanetary electric fields and polar cap potential drop are much larger than the ratios for prompt penetration events shown in Figures 2, 3, and 4 which indicates the magnitudes of the prompt penetration electric fields are strongly local time dependent. These observations were still under the effects of the recovery phase of a severe magnetic storm. After 1000 UT on 12 November, the Jicamarca vertical drifts closely matched their average quiet time values.

4. Discussion

[29] We have seen that large and highly variable equatorial electric field perturbations were often observed during the November 2004 storm. In this section, we summarize our results and discuss their implications on the present understanding of equatorial storm-time electric fields focusing mostly on prompt penetration electric fields, which have been the subject of considerable recent interest.

[30] Our observations clearly indicate that, in general, the equatorial perturbation electric fields are not proportional to the solar wind and reconnection electric fields and polar cap potential drops. In particular, the measurements during 7 November showed large eastward and westward electric fields during the storm main phase, when the solar wind and

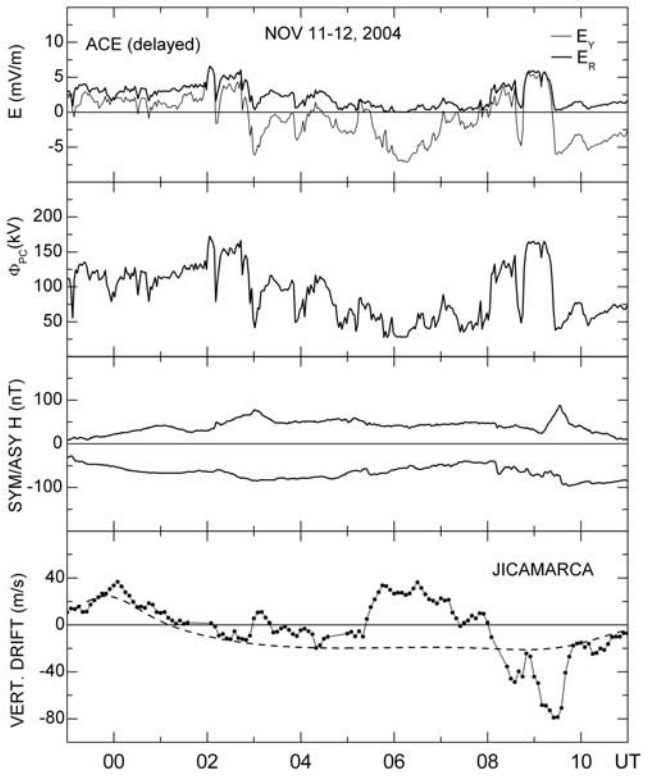

Figure 6. Solar wind electric fields, polar cap potential drops, *SYM-H* and *ASY* indices, and Jicamarca vertical drifts during 11–12 November 2004. The dashed curve denotes the quiet time drift pattern.

reconnection eastward electric fields, and the estimated polar cap potential drop all had large and nearly steady magnitudes. In addition, our data did not show polar cap saturation effects on the perturbation electric fields. During the 9 November storm main phase, the equatorial eastward electric fields perturbations had lifetimes of about one hour, but they were not proportional to the solar wind electric fields and polar cap potential drop. These results are not consistent with recent suggestions [e.g., *Huang et al.*, 2005, 2007; *Maruyama et al.*, 2007] that during storm main phase the solar wind electric fields penetrate without attenuation into the equatorial ionosphere for several hours. On the other hand, our observations confirm that prompt penetration electric fields are associated with large and rapid changes in the interplanetary electric fields, which has been known for several years [e.g., *Kelley et al.*, 1979; *Gonzales et al.*, 1979; *Fejer*, 1986].

[31] The relationship of rapid IMF *Bz* changes and nearly simultaneous short-lived electric field and ionospheric current perturbations from high to equatorial latitudes has been studied for several years [e.g., *Kelley et al.*, 1979; *Gonzales et al.*, 1979; *Fejer*, 1986; *Kikuchi et al.*, 1996]. Recently, *Kelley et al.* [2003] showed that, for periods less than about 2 h during 15-18 April 2002 the ratio of the equatorial and interplanetary dawn-to-dusk electric field components was about 0.07. *Huang et al.* [2007] used extensive daytime Jicamarca vertical drift and ACE solar wind observations to derive an empirical value of 9.6% for this penetration efficiency. Although, we have not done a detailed study of this ratio, our data are consistent with an average daytime value of about 0.05–0.1, but they also clearly show that this ratio is highly variable even during the day. Furthermore, we have also seen that this ratio was about 0.25 shortly before UT dawn on 12 November, which is fully consistent with the occurrence of significantly larger nighttime prompt penetration perturbations drifts reported in earlier studies [e.g., *Gonzales et al.*, 1979; *Fejer*, 1986; *Fejer et al.*, 1990; *Fejer and Emmert*, 2003]. Figures 4 and 6 in *Gonzales et al.* [1979], for example, show much larger simultaneous prompt penetration electric field effects in the nightside equatorial ionosphere than in the dayside.

[32] As shown by numerous modeling studies, the morphology and physics of equatorial prompt penetration electric fields are far more complex than implied by simple proportionality factors between the either the magnitudes or the time rate of changes of equatorial and solar wind electric fields [e.g., *Jaggi and Wolf*, 1973; *Senior and Blanc*, 1984; *Wolf et al.*, 1982; *Spiro et al.*, 1988; *Fejer et al.*, 1990; *Peymirat et al.*, 2000; *Tsunomura*, 1999; *Sazykin*, 2000; *Richmond et al.*, 2003; *Rothwell and Jasperse*, 2006]. These studies have shown that the prompt penetration effects are driven by the solar wind and magnetospheric driving mechanisms, but that their strength, duration and local time dependence are controlled by the potential distribution penetrating to middle and low latitudes, which depend on magnetospheric parameters such as the equivalent ring current conductivity (proportional to the plasma sheet temperature and density), and on ionospheric conductances. The enhancements of the prompt penetration electric field near sunrise and sunset, for example, are mostly due to day-to-night conductivity changes.

[33] Theoretical and numerical model studies suggest that the shielding time constant is generally of the order of 20 min, but that it can vary between about 5 and 200 min, depending on magnetospheric plasma properties and ionospheric conductivities [e.g., *Jaggi and Wolf*, 1973; *Wolf et al.*, 1982; *Senior and Blanc*, 1984; *Peymirat et al.*, 2000]. These models indicate that shielding is stronger when the plasma sheet is cold and dense and weaker when it is hot and rarefied [*Spiro et al.*, 1988; *Garner et al.*, 2004]. In addition, they can potentially undergo large variations due to changes in the magnetic field geometry in the magnetotail, which are controlled by the cross tail current [*Fejer et al.*, 1990; *Sazykin*, 2000].

[34] Several studies have presented examples of equatorial electric field fluctuations with time constants of about an hour and lasting for several hours during geomagnetic disturbed conditions [e.g., *Gonzales et al.*, 1979; *Kelley et al.*, 2003]. Since these events occur invariably during periods of corresponding fluctuations in the solar wind and magnetospheric driving processes, they result from a series of short-lived prompt penetration electric field and not from single long-lived ones.

5. Conclusions

[35] The November 2004 magnetic storm produced large and complex electrodynamic disturbances in the equatorial ionosphere, which were well suited for testing the present understanding of the response of low latitude ionospheric electric fields to strongly enhanced geomagnetic activity.

[36] We have seen that before the storm onset, large equatorial prompt penetration and disturbance dynamo electric fields occurred following large solar wind eastward electric field and polar cap potential drop increases. During storm main phase, when the IMF *Bz*, the solar wind E_y, and reconnection eastward electric fields, and polar cap potential drop all had very large magnitudes, the equatorial daytime measurements showed large and rapidly varying eastward and westward current perturbations, which were generally associated with changes in the time rate of change of the *Dst* index. These large electric fields perturbations are inconsistent with the suggestion that, the equatorial prompt penetration zonal electric fields are proportional to the solar wind electric fields and have long lifetimes during storm main phase.

[37] The largest prompt penetration vertical plasma drift perturbations (about 120 m/s) ever observed over Jicamarca occurred in the afternoon of 9 November 2004, following rapid increases in the solar wind electric field by about 30 mV/m, and in the cross polar cap potential by about 250 kV. These perturbation electric fields were consistent with simultaneous equatorial electrojet current disturbances in the Pacific and ionosonde drift perturbations over Brazil. The rapid decrease of the solar wind and polar cap potential after this strong prompt penetration event resulted in equatorial westward electric fields lasting about 4 h, which were mostly due to disturbance dynamo effects. Large magnitude short-lived prompt penetration and long lasting disturbance dynamo electric fields were observed on the nightside over Jicamarca and in the dayside in the Pacific during November 10. In this case, disturbance dynamo electric fields largely dominated the equatorial electric field response

in spite of the very large, but mostly steady, solar wind electric fields, and polar cap potential drops.

[38] Large prompt penetration electric fields were present over Jicamarca near dawn during 12 November. In this case, the ratio of the equatorial westward prompt penetration electric fields and change in solar wind and reconnection electric fields was about 3 times larger than during the afternoon of 9 November storm main phase, which show that these ratios varied considerably during this large storm. Our data are consistent with earlier experimental and model studies which indicated that the magnitude of the prompt penetration electric fields is local time dependent and that they have strong dependence on magnetospheric (e.g., ring current ion pressure), and ionospheric parameters (e.g., conductances).

[39] The results presented here clearly highlight that under severe storm conditions, the relationship of equatorial prompt penetration electric fields and solar wind electric field effects and solar wind and reconnection electric field and polar cap potential drops is far more complex than implied by simple proportionality factors. They also show that the understanding of equatorial storm-time electric fields require more detailed studies using global ionospheric measurements and extensive numerical modeling.

[40] **Acknowledgments.** We thank R. Wolf for very helpful discussions, and the referees for helpful comments. The magnetometer data from Yap and Okinawa are due to the space weather monitoring system of the National Institute of Information and Communication Technology (NICT) of Japan. The work at Utah Sate University was supported by Aeronomy Program, Division of Atmospheric Sciences through grant ATM-0534038, and by the National Aeronautics and Space Administration through grant NAG5-8638. The Jicamarca Radio Observatory is a facility of the Instituto Geofisico del Peru and is operated with support from the NSF Cooperative Agreement ATM-0432565 through Cornell University.

[41] Amitava Bhattacharjee thanks J. Ruohoniemi and Eurico de Paula for their assistance in evaluating this paper.

References

Abdu, M. A., I. S. Batista, G. O. Walker, J. H. A. Sobral, N. B. Trivedi, and E. R. de Paula (1995), Equatorial ionospheric electric fields during magnetospheric disturbances: Local/longitudinal dependencies from recent EITS campaigns, *J. Atmos. Sol. Terr. Phys.*, *57*, 1065.

Anderson, D., A. Anghel, K. Yumoto, M. Ishitsuka, and E. Kudeki (2002), Estimating daytime vertical E × B drift velocities in the equatorial *F*-region using ground-based magnetometer observations, *Geophys. Res. Lett.*, *29*(12), 1596, doi:10.1029/2001GL015462.

Basu, S., Su Basu, K. M. Groves, H-.C. Yeh, S.-Y. Su, F. J. Rich, P. J. Sultan, and M. J. Keskinen (2001), Response of the equatorial ionosphere in the South Atlantic region to the magnetic storm of July 15, 2000, *Geophys. Res. Lett.*, *18*, 3577.

Bittencourt, J. A., and M. A. Abdu (1981), A theoretical comparison between apparent and real vertical ionization drift velocities in the equatorial *F* region, *J. Geophys. Res.*, *86*, 2451.

Blanc, M., and A. D. Richmond (1980), The ionospheric disturbance dynamo, *J. Geophys. Res.*, *85*, 1669.

Boyle, C. B., P. H. Reiff, and M. R. Hairston (1997), Empirical polar cap potentials, *J. Geophysl Res.*, *102*, 111.

Buonsanto, M. J. (1999), Ionospheric storms: A review, *Space Sci. Rev.*, *88*, 563.

Fejer, B. G. (1986), Equatorial ionospheric electric fields associated with magnetospheric disturbances, in *Solar Wind-Magnetosphere Coupling*, edited by Y. Kamide and J. A. Slavin, pp. 519–545, Terra Sci., Tokyo.

Fejer, B. G. (1997), The electrodynamics of the low-latitude ionosphere: Recent results and future challenges, *J. Atmos. Sol.-Terr. Phys.*, *59*, 1465.

Fejer, B. G. (2002), Low latitude storm time ionospheric electrodynamics (2002), *J. Atmos. Sol.-Terr. Phys.*, *64*, 1401.

Fejer, B. G. (2004), Solar wind-magnetosphere effects in the middle and low latitude ionosphere, in *Auroral Phenomena and Solar Terrestrial Relations*, edited by L. Zeleyi and M. Geller, and J. Allen, CAWSES Handbook-1, Boulder, CO.

Fejer, B. G., and L. Scherliess (1997), Empirical models of storm time equatorial electric fields, *J. Geophys. Res.*, *102*, 24,047.

Fejer, B. G., and J. T. Emmert (2003), Low-latitude ionospheric disturbance electric field effects during the recovery phase of the 19-21 October 1998 magnetic storm, *J. Geophys. Res.*, *108*(A12), 1454, doi:10.1029/2003JA010190.

Fejer, B. G., R. W. Spiro, R. A. Wolf, and J. C. Foster (1990), Latitudinal variation of perturbation electric fields during magnetically disturbed periods: 1986 SUNDIAL observation and model results, *Ann. Geophys.*, *8*, 441.

Fuller-Rowell, T. J., G. H. Millward, A. D. Richmond, and M. V. Codrescu (2002), Storm-time changes in the upper atmosphere at low latitudes, *J. Atmos. Sol.-Terr. Phys.*, *64*, 1383.

Garner, T. W., R. A. Wolf, R. W. Spiro, W. J. Burke, B. G. Fejer, S. Sazykin, J. L. Roeder, and M. R. Hairston (2004), Magnetospheric electric fields and plasma sheet injection to low-L shells during the 45 June 1991 magnetic storm: Comparison between the Rice Convection Model and observations, *J. Geophys. Res.*, *109*, A02214, doi:10.1029/2003JA010208.

Gonzales, C. A., M. C. Kelley, B. G. Fejer, J. F. Vickrey, and R. F. Woodman (1979), Equatorial electric fields during magnetically disturbed conditions 2. Implications of simultaneous auroral and equatorial measurements, *J. Geophys. Res.*, *84*, 5803.

Huang, C. S., J. C. Foster, and M. C. Kelley (2005), Long-duration penetration of interplanetary electric field to the low latitude ionosphere during the main phase of magnetic storms, *J. Geophys. Res.*, *110*, A11309, doi:10.1029/2005JA011202.

Huang, C. S., S. Sazykin, J. L. Chau, N. Maruyama, and M. C. Kelley (2007), Penetration electric fields: Efficiency and characteristic time scale, *J. Atmos. Sol. Terr. Phys.*, doi:10.1016/j.jastp.2006.08.06.

Iyemori, T. (1990), Storm-time magnetospheric currents inferred from mid-latitude geomagnetic field variation, *J. Geomagn. Geoelectr.*, *42*, 1249.

Iyemori, T., and D. R. K. Rao (1996), Decay of the Dst field of geomagnetic disturbance after substorm onset and its implication to storm-substorm relation, *Ann. Geophys.*, *14*, 618.

Jaggi, R. K., and R. A. Wolf (1973), Self-consistent calculation of the motion of a plasma sheet of ions in the magnetosphere, *J. Geophys. Res.*, *78*, 2852.

Kelley, M. C. (1989), *The Earth's Ionosphere, Plasma Physics and Electrodynamics*, Academic, San Diego, Calif.

Kelley, M. C., B. G. Fejer, and C. A. Gonzales (1979), An explanation for anomalous ionospheric electric fields associated with a northward turning of the interplanetary magnetic field, *Geophys. Res. Lett.*, *6*, 301.

Kelley, M. C., J. J. Makela, J. L. Chau, and M. J. Nicholls (2003), Penetration of the solar wind electric field into the magnetosphere/ionosphere system, *Geophys. Res. Lett.*, *30*(4), 1158, doi:10.1029/2002GL016321.

Kikuchi, T., H. Luhr, T. Kitamura, O. Saka, and K. Schlegel (1996), Direct penetration of the polar electric field to the equator during a DP2 event as detected by the auroral and equatorial magnetometer chains and the EISCAT radar, *J. Geophys. Res.*, *101*, 19,643.

Kikuchi, T., H. Luhr, K. Schlegel, H. Tachihara, M. Shinohara, and T.-I. Kitamura (2000), Penetration of auroral electric fields to the equator during a substorm, *J. Geophys. Res.*, *105*, 23,251.

Kikuchi, T., K. K. Hashimoto, T.-I. Kitamura, H. Tachihara, and B. Fejer (2003), Equatorial counter electrojets during a substorms, *J. Geophys. Res.*, *108*(A11), 1406, doi:10.1029/2003JA009915.

Kudeki, E., and C. Fawcett (1993), High resolution observations of 150 km echoes at Jicamarca, *Geophys. Res. Lett.*, *20*, 1987.

Kudeki, E., S. Bhattacharyya, and R. F. Woodman (1999), A new approach in incoherent scatter *F* region E × B drift measurements at Jicamarca, *J. Geophys. Res.*, *104*, 28,145.

Maruyama, N., A. D. Richmond, T. J. Fuller-Rowell, M. V. Codrescu, S. Sazykin, F. R. Toffoletto, R. W. Spiro, and G. H. Millward (2005), Interaction between direct penetration and disturbance dynamo electric fields in the storm-time equatorial ionosphere, *Geophys. Res. Lett.*, *32*, L17105, doi:10.1029/2005GL023763.

Maruyama, N., S. Sazykin, R. W. Spiro, R. A. Wolf, D. Anderson, A. Anghel, F. R. Toffoletto, T. J. Fuller-Rowell, M. V. Codrescu, and G. H. Millward (2007), Modeling storm-time electrodynamics of the low latitude ionosphere-thermosphere system: Can long lasting disturbance electric fields be accounted for?, *J. Atmos. Sol. Terr. Phys*, doi:10.1016/j.jastp.2006.08.020.

Ober, D. M., N. C. Maynard, and W. J. Burke (2003), Testing the Hill model of the transpolar potential saturation, *J. Geophys. Res.*, *108*(A12), 1467, doi:10.1029/2003JA010154.

Peymirat, C., A. D. Richmond, and A. T. Kobea (2000), Electrodynamic coupling of high and low latitudes: Simulations of shielding/overshielding effects, *J. Geophys. Res.*, *105*, 22,991.

Richmond, A. D., C. Peymirat, and R. G. Roble (2003), Long-lasting disturbances in the equatorial ionospheric electric field simulated with

a coupled magnetosphere-ionosphere-thermosphere model, *J. Geophys. Res.*, *108*(A3), 1118, doi:10.1029/2002JA009758.

Rothwell, P. L., and J. R. Jasperse (2006), Modeling the connection of the global ionospheric electric fields to the solar wind, *J. Geophys. Res.*, *111*, A03211, doi:10.1029/2004JA010992.

Sastri, J. H., M. A. Abdu, and J. H. A. Sobral (1997), Response of equatorial ionosphere to episodes of asymmetric ring current activity, *Ann. Geophys.*, *15*, 1316.

Sastri, J. H., K. Niranjan, and K. S. V. Subbarao (2002), Response of the equatorial ionosphere in the Indian (midnight) sector to the severe magnetic storm of July 15, 2000, *Geophys. Res. Lett.*, *29*(13), 1651, doi:10.1029/2002GL015133.

Sazykin, S. (2000), Theoretical studies of penetration of magnetospheric electric fields to the ionosphere, PhD dissertation, 292 pp., Utah State Univ., Logan.

Scherliess, L., and B. G. Fejer (1997), Storm time dependence of equatorial disturbance dynamo zonal electric fields, *J. Geophys. Res.*, *102*(A12), 24,037.

Senior, C., and M. Blanc (1984), On the control of magnetospheric convection by the spatial distribution of ionospheric conductivities, *J. Geophys. Res.*, *89*, 261.

Siscoe, G. L., G. M. Erickson, B. U. O. Sonnerup, N. C. Maynard, J. A. Schoendorf, D. R. Weimer, and G. R. Gordon (2002), Hill model of the transpolar potential saturation: Comparison with MHD simulations, *J. Geophys. Res.*, *107*(A6), 1075, doi:10.1029/2001JA000109.

Spiro, R. W., R. A. Wolf, and B. G. Fejer (1988), Penetration of high-latitude electric fields effects to low latitudes during SUNDIAL 1984, *Ann. Geophys.*, *6*, 39.

Su, S-.Y., C. K. Chao, H. C. Yeh, and R. A. Heelis (2003), Observations of shock impact, disturbance dynamo, and a midlatitude large-density depletion at 600 km altitude on the 17 April 2002 storm, *J. Geophys. Res.*, *108*(A8), 1310, doi:10.1029/2002JA009752.

Tsunomura, S. (1999), Numerical analysis of global ionospheric current system including the effect of the equatorial enhancement, *Ann. Geophysicae*, *17*, 692.

Wolf, R. A. (1983), The quasi-static (slow flow) region of the magnetosphere, in *Solar Terrestrial Physics*, R. L. Carovilano and J. M. Forbes (Eds.), D. Reidel, Hingahm, MA., pp. 303–368.

Wolf, R. A., R. W. Spiro, S. Sazykin, and F. R. Toffoleto (2007), How the Earth's inner magnetosphere works: An evolving picture, *J. Atmos. Sol.-Terr. Phys.*, *69*, 288.

Wolf, R. A., R. W. Spiro, G.-H. Voigt, P. H. Reiff, C. K. Chen, and M. Harel (1982), Computer simulation of inner magnetospheric dynamics for the magnetic storm of July 29, 1977, *J. Geophys. Res.*, *87*, 5949.

Woodman, R. F. (1970), Vertical drifts and east-west electric fields at the magnetic equator, *J. Geophys. Res.*, *75*, 6249.

Woodman, R. F., and F. Villanueva (1995), Comparisons of electric fields measured at F-region heights with 150-km irregularity drift measurements, paper presented at the Ninth International Symposium on Equatorial Aeronomy, Natl. Sci., Found., Bali, Indonesia.

M. A. Abdu, Instituto de Pesquisas Espaciais, 12227-010 Sao Jose dos Campos, SP, Brazil.

J. L. Chau, Radio Observatorio de Jicamarca, Instituto Geofisico del Peru, Peru.

B. G. Fejer and J. W. Jensen, Center for Atmospheric and Space Science, Utah State University, Logan, UT 94322-4405, USA. (bfejer@cc.usu.edu)

T. Kikuchi, Solar Terrestrial Environment Laboratory, Nagoya University, Nagoya, Aichi 464-8601, Japan.